Comparative study of optical phonons in the rhombohedrally distorted perovskites $LaAlO_3$ and $LaMnO_3$

M. V. Abrashev,* A. P. Litvinchuk, M. N. Iliev, and R. L. Meng
Texas Center for Superconductivity, University of Houston, Houston, Texas 77204-5932

V. N. Popov and V. G. Ivanov
Faculty of Physics, Sofia University, BG-1164 Sofia, Bulgaria

R. A. Chakalov
Institute of Electronics, Bulgarian Academy of Sciences, Tzarigradsko Chausse 72, 1784 Sofia, Bulgaria

C. Thomsen
Institut für Festkörperphysik, Technische Universität Berlin, Hardenbergstrasse 36, D-10623 Berlin, Federal Republic of Germany
(Received 10 August 1998)

The Raman and infrared phonons of isostructural rhombohedral $LaMnO_3$ and $LaAlO_3$ are studied at room temperature. The experimental spectra are compared with the prediction of lattice-dynamical calculations and the lines observed are assigned to definite atomic vibrations. It is shown that the Raman mode of A_{1g} symmetry in $LaAlO_3$ and $LaMnO_3$ (at 123 cm^{-1} and 236 cm^{-1}, respectively) involves atomic motions that cause the rhombohedral distortion, i.e., it is a ''soft'' mode, and its position could be used as a measure of the degree of the distortion. It is also argued that the broad Raman bands in the high-frequency range of $LaMnO_3$ are not proper modes of the rhombohedral $R\bar{3}c$ structure, but are rather induced by the dynamic Jahn-Teller effect. [S0163-1829(99)02706-X]

I. INTRODUCTION

The manganese perovskites with general formula $R_{1-x}A_xMnO_3$ (R = rare earth, A = Ca, Sr, Ba, Pb) are characterized by a strong interplay of the structural, electronic, and magnetic properties. Recently, they attracted a renewed interest due to the effect of ''colossal'' negative magnetoresistance (CMR) exhibited near the temperature where metal-insulator and paramagnetic-ferromagnetic transitions occur.[1] Shortly after the discovery of these materials, the concept of the ''double-exchange'' (DE) has been developed to describe both the ferromagnetism (FM) and the metallic conductivity in the low-temperature phase. Within the DE model the transport in the FM metallic phase involves hopping of spin-polarized charge between Mn^{3+} and Mn^{4+} sites.[2] However, recently Millis *et al.*[3] have shown that the DE alone is insufficient to account for either the low transition temperature or the large change in resistivity near T_c. It has been proposed that in addition to the DE mechanism, the strong electron-phonon coupling in the form of dynamical Jahn-Teller distortions tends to localize the conduction electrons into polaronic states. While the Jahn-Teller distortions are large in the insulating state, they are at least partly removed below T_c. The large isotope shift of T_c ($\sim$20 K) upon ^{18}O for ^{16}O substitution does indicate a strong spin-lattice coupling.[4] Therefore it is expected that the Raman and infrared spectroscopies could be powerful tools to clarify the role of the phonons in CMR and related phenomena.

The crystal structure of the undoped parent compound $LaMnO_3$ depends on the synthesis conditions.[5,6] At least two well-determined phases exist at room temperature: the orthorhombically distorted (space group $Pnma$) and the rhombohedrally distorted (space group $R\bar{3}c$), both are paramagnetic insulators.[6] The rhombohedral phase is of special interest as it is typical for some $R_{1-x}A_xMnO_3$ materials exhibiting CMR. It is plausible to expect the phonon spectra of this phase to be sensitive to some specific features associated with the CMR. Such are the variations of Jahn-Teller distortions with the Mn^{4+}/Mn^{3+} ratio as well as with the temperature near T_c. The phonon spectra will also be sensitive to the degree of rhombohedral distortions. This concerns, in particular, the first-order Raman spectra, which become allowed exclusively due to lattice distortions as no Raman-active modes are anticipated in the ideal perovskite structure ($Pm\bar{3}m$). At present there is, however, scanty data on the Raman spectra of rhombohedral $LaMnO_3$ and related $La_{1-x}A_xMnO_3$ compounds and the assignment of the observed spectral structures is still ambiguous. The main difficulties arise because of the very low Raman intensities, which has given rise to speculations that some of the broad bands in the experimental spectra may correspond to second-order Raman processes.[7] To our knowledge there are no reports on either polarized Raman spectra of rhombohedral $LaMnO_3$ that could unambiguously determine the symmetries of experimentally observed lines, or on lattice dynamical calculations (LDC) that could predict the shapes of Raman modes of given symmetry and the expected range of their wave numbers.

In this work we report the results of our study of optical phonons in isostructural rhombohedral $LaMnO_3$ and

TABLE I. Calculated wave numbers (in cm^{-1}) of even- (upper part) and odd-parity (lower part) phonon modes in rhombohedral $LaAlO_3$ and $LaMnO_3$ and their assignment. The corresponding R- and Γ-point modes of the parent cubic structure ($Pm3m$) are listed in the last column. A_{2g} and A_{1u} modes are silent.

	$LaAlO_3$			$LaMnO_3$			
A_{1g}	A_{2g}	E_g	A_{1g}	A_{2g}	E_g	Assignment	Modes in $Pm3m$
132		34	249		42	Rotational	$F_{2u}(R)$
	158	163		139	163	La	$F_{1u}(R)$
	456	463		441	468	Bending	$F_{1u}(R)$
		691			646	Antistretching	$E_u(R)$
	742			716		Breathing	$A_{2u}(R)$
A_{1u}	A_{2u} TO/LO	E_u TO/LO	A_{1u}	A_{2u} TO/LO	E_u TO/LO		
480		481/505	320		317/326	Al/Mn	$F_{2g}(R)$
	213/263	220/263		162/216	180/213	(Al/Mn + O) La	$F_{1u}(\Gamma)$
	366/496	371/475		310/465	357/488	Bending	$F_{1u}(\Gamma)$
	706/712	707/712		641/645	642/645	Stretching	$F_{1u}(\Gamma)$
299		270/270	361		240/241	Torsional	$F_{2u}(\Gamma)$

$LaAlO_3$. The experimental Raman and infrared spectra are analyzed by comparison with the prediction of lattice-dynamical calculations. We show that the Raman mode of A_{1g} symmetry at 123 cm^{-1} and 236 cm^{-1} for $LaAlO_3$ and $LaMnO_3$, respectively, involves atomic motions that cause the rhombohedral distortion, i.e., it is a ''soft'' mode, and its position could be used as a measure of the degree of the distortion. We also argue that the broad Raman bands in the high-frequency phonon range of $LaMnO_3$ are not proper modes of the $R3c$ structure, but are rather induced by the dynamic Jahn-Teller effect. All experimentally observed lines in the infrared spectra of $LaMnO_3$ and $LaAlO_3$ are also assigned to definite atomic vibrations.

II. SAMPLES AND EXPERIMENT

The $LaAlO_3$ single crystal investigated was a commercially available product (CrysTec GmbH, Berlin, Germany) with platelike shape ($5\times5\times0.5$ mm^3) and edges parallel to the quasicubic crystallographic axes. The observation of the crystal surface under microscope using white linearly polarized light revealed a twinned structure with averaged twin size of about 20 μm. The preparation of the rhombohedral $LaMnO_3$ ceramics is described elsewhere.[8] For the latter material the spectra were taken from the polished surface containing optically isotropic grains of irregular shape.

The Raman spectra were measured using a LabRam single spectrometer equipped with appropriate notch filters, an optical microscope and CCD detector. An $\times100$ objective was used to both focus the incident laser beam into a spot of 1–2 μm in diameter and collect the scattered light in backward-scattering geometry. The 632.8-nm He-Ne laser line was used for excitation.

The near-normal incidence infrared reflectance spectra were measured with a Bomem DA8 Fourier-transform interferometer in the range 50–8000 cm^{-1}, using a gold mirror as a reference. All measurements were performed at room temperature.

III. RESULTS AND DISCUSSION

A. Classification of the Γ-point phonons

The rhombohedral $LaMO_3$ (M = Al, Mn) has the symmetry of the space group $R3c$ (D_{3d}^6, Z=2) and belongs to the family of rotationally distorted perovskites with Glazer's notation ($a^-a^-a^-$).[9] The $R3c$ structure can be obtained from the simple-cubic perovskite ($Pm3m$) by rotation of the adjacent MO_6 octahedra in opposite directions around the $[111]_c$ (cubic) direction. In the $R3c$ lattice the La atoms occupy the $2a$ ($\frac{1}{4},\frac{1}{4},\frac{1}{4}$) positions and participate in four Γ-point phonon modes ($A_{2g}+A_{2u}+E_g+E_u$). The M (M = Al, Mn) atoms occupy the $2b$ (0,0,0) positions and also participate in four modes ($A_{1u}+A_{2u}+2E_u$). The oxygen atoms occupy the $6e$ ($x,x+\frac{1}{2},\frac{1}{4}$) positions and take part in twelve modes ($A_{1g}+A_{1u}+2A_{2g}+2A_{2u}+3E_g+3E_u$). Of the total 20 Γ-point modes 18 correspond to optical phonons. The $A_{1g}+4E_g$ modes are only Raman active, the $3A_{2u}+5E_u$ are only infrared active, and the remaining $2A_{1u}+3A_{2g}$ modes are inactive (''silent'') modes. For better understanding of the relationship between the frequency and vibrational patterns of the modes investigated it is instructive to recall the correlation between the modes in distorted $R3c$ and undistorted $Pm3m$ structures (see, e.g., Scott[10]). The tilts of the octahedra result in doubling of the cubic unit cell and therefore the Γ_r-point phonon modes of the rhombohedral Brillouin zone come from modes located at the Γ_c (0,0,0) and R_c ($\frac{1}{2},\frac{1}{2},\frac{1}{2}$) points of the cubic Brillouin zone. Additionally, the triply degenerated modes of the cubic structure split into pairs of nondegenerated and doubly degenerated modes in the rhombohedral structure (see Table I).

The selection rules for the Raman-active modes are represented by the following tensors:[11]

TABLE II. Expected intensity of the Raman-active phonons in the experimentally available polarizations.

Symmetry	Polarization $xx \equiv yy$	xy	$x'x'$	$y'y'$	$x'y'$
A_{1g}	$\frac{1}{9}(2a+b)^2$	$\frac{1}{9}(b-a)^2$	a^2	$\frac{1}{9}(a+2b)^2$	0
E_g	$\frac{1}{9}(1+\sqrt{3})(c+\sqrt{2}d)^2$	$\frac{1}{9}(-2c+\sqrt{2}d)^2$	c^2	$\frac{1}{9}(-c+2\sqrt{2}d)^2$	$\frac{1}{3}(c+\sqrt{2}d)^2$

$$A_{1g}=\begin{pmatrix} a & 0 & 0 \\ 0 & a & 0 \\ 0 & 0 & b \end{pmatrix}; \quad E_{g,1}=\begin{pmatrix} c & 0 & 0 \\ 0 & -c & d \\ 0 & d & 0 \end{pmatrix}; \quad E_{g,2}=\begin{pmatrix} 0 & -c & -d \\ -c & 0 & 0 \\ -d & 0 & 0 \end{pmatrix}, \tag{1}$$

given in a standard orthogonal basis O_x, O_y, O_z. This basis is related to the hexagonal unit cell, which is alternatively used to describe the $R\bar{3}c$ structure, as follows: $O_z \| \mathbf{c}_h$, $O_x \| \mathbf{a}_h$, where $\mathbf{a}_h$, $\mathbf{b}_h$, and $\mathbf{c}_h$ are the unit vectors of the hexagonal cell.

The naturally grown surfaces of the perovskitelike crystals are the quasicubic $(100)_c$ ones. From such surfaces one can obtain Raman spectra in the following backward scattering configurations (see the inset of Fig. 2): xx, yy, xy, $x'x'$, $y'y'$, and $x'y'$, where x, y, x', and y' are the quasicubic $[100]_c$, $[010]_c$, $[1\bar{1}0]_c$, and $[110]_c$ directions, respectively. The expected intensities of the Raman lines with these configurations are listed in Table II.

B. Description of the model used for lattice-dynamical calculations (LDC)

The model applied for calculations of the lattice dynamics was a shell model with parameters derived as described in Ref. 12. The model is appropriate for the perovskitelike oxides as, in accordance with their predominant ionicity, the interionic interactions can be represented as sums of long-range Coulomb potentials and short-range potentials. The latter were chosen in the Born-Mayer-Buckingham form

$$V = a \exp(-br) - \frac{c}{r^6}, \tag{2}$$

where a, b, and c are parameters, and r is the interionic separation. The ionic polarizability is also accounted for using the simple picture of an ion as a point-charged core coupled with a force constant k to a charged massless shell with charge Y around it. The free-ion polarizability α is given by

$$\alpha = \frac{Y^2}{k}. \tag{3}$$

The values of model parameters (listed in Table III) were close to those used in LDC of orthorhombic $(Pnma)$ $LaMnO_3$.[8] The crystallographic data for $LaAlO_3$ and $LaMnO_3$ have been taken from Refs. 14 and 6, respectively. The calculated frequencies of the optical phonons in $LaMO_3$ $(M = \mathrm{Al, Mn})$ are presented in Table I. The corresponding vibrational patterns are drawn in Fig. 1.

C. Raman spectroscopy

The polarized Raman spectra of $LaAlO_3$ as obtained from a large twin on the quasicubic $(001)_c$ surface are shown in Fig. 2. Three strong lines at 123, 152, and 487 cm^{-1} dominate the spectra. Based on their polarization properties and our LDC we assign them to the calculated A_{1g} mode at 132 cm^{-1} (rotation of the oxygen octahedra around the hexagonal $[001]_h$ direction), E_g mode at 163 cm^{-1} [pure La vibration in the hexagonal $(001)_h$ plane] and E_g mode at 463 cm^{-1} (pure oxygen bending vibration), respectively. The line corresponding to the calculated E_g mode at 691 cm^{-1} (out-of-phase stretching oxygen vibration) was not observed, which indicates that it may be of negligible intensity. The remaining expected E_g mode (rotation of the oxygen octahedra around an axis perpendicular to the hexagonal $[001]_h$ direction with calculated Raman shift of 34 cm^{-1}) is very close to the laser line and couldnot be detected with our setup.

It is worth noting that our experimental results are in excellent agreement with those of the pioneer work of Scott.[10] In that paper the low-frequency E_g mode at 33 cm^{-1} (at room temperature) had also been observed. The line near 150 cm^{-1}, however, had been interpreted as a ''ghost'' line and the very weak line near 470 cm^{-1} as a E_g mode. The latter line (also very weak) is observed in our spectra, too, with polarization properties as for the two other E_g lines. As

TABLE III. Parameters used in the shell model. The short-range O-O potential is taken from Ref. 13.

Ion	Z ($\|e\|$)	Y ($\|e\|$)	α (Å^3)	Ionic pair	a (eV)	b (Å^{-1})	c (eV Å^6)
La	2.85	1.7	0.7	La-O	1563	2.734 [a]/2.748 [b]	0
Al	2.85	1.7	0.6	Al-O	1838	3.345	0
Mn	2.85	3.0	3.0	Mn-O	2020	3.345	0
O	−1.90	−3.0	2.0	O-O	22764	6.710	20.37

[a]For $LaAlO_3$.
[b]For $LaMnO_3$.

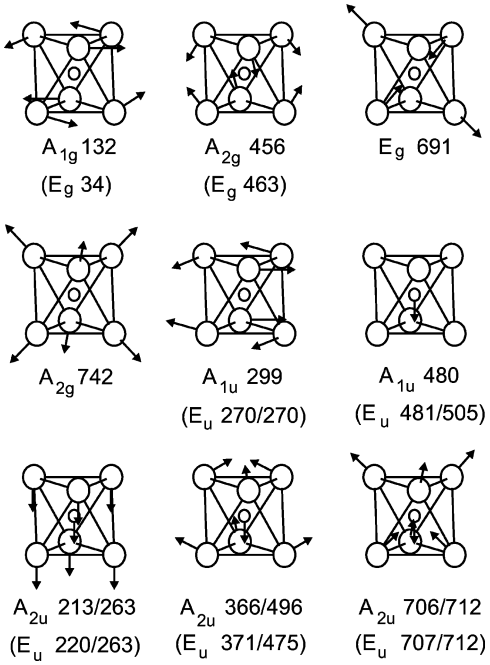

FIG. 1. The calculated vibrational patterns of the optical phonons in $LaAlO_3$. One oxygen octahedron is drawn only. The hexagonal c axis (parallel to C_3) is vertical. Due to the similarity of the vibrational shapes of the pair modes, originated from triply degenerated modes in the cubic structure, the vibrational pattern of the nondegenerated A-type modes is drawn only.

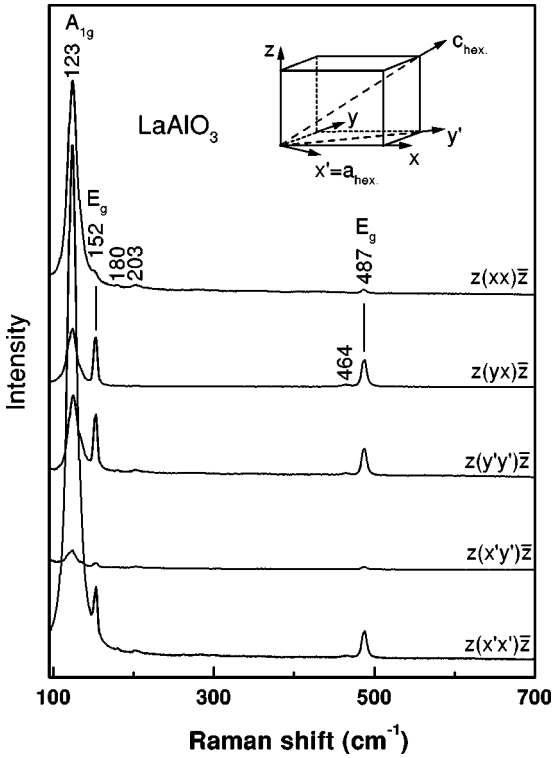

FIG. 2. Polarized Raman spectra in different scattering configurations obtained from a twin with quasi-cubic [100] surface of $LaAlO_3$ single crystal. The inset shows the symbols used for the different crystal directions. $\lambda_L = 632.8$ nm.

long as only one Raman phonon is predicted by the LDC in this frequency range, we suppose that the weak line at 464 cm^{-1} (E_g), as well as two other weak lines at 180 and 203 cm^{-1} (with the same polarization properties as the 123-cm^{-1} A_{1g} line) do not originate from Raman-allowed one-phonon scattering.

By comparison of experimentally measured relative intensities of the three strong Raman lines with those expressed in terms of the elements of the Raman tensors (see Table II) one can determine the relative values of the nonzero elements of corresponding Raman tensors. The two E_g lines are of equal intensity with yx, $y'y'$, and $x'x'$ polarization configurations, but are of negligible intensity with the xx and $x'y'$ configurations. It follows from Table II that this is possible if $d=-c/\sqrt{2}$. For the A_{1g} line the ratio of the intensities with $x'x'$, xx, yx, and $y'y'$ is close to 9:4:1:1, which requires the inequality $a \gg b$ to be satisfied. We suggest that the similar relationships between the Raman tensor elements would hold for the isostructural $LaMnO_3$, too.

As concerns the rhombohedral $LaMnO_3$, let us first outline the experimental difficulties in obtaining the Raman spectra.

(a) The $LaMnO_3$ ceramic sample used consisted of optically isotropic grains of irregular shape. The Raman spectra taken at various spots on the surface were identical and, moreover, independent on the polarization direction of the incident laser light. This could be due to a fine twinning and/or to the submicron size of the microcrystals. It was, therefore, possible to obtain only two types spectra: with parallel ($e_i \| e_s$) and crossed ($e_i \perp e_s$) polarizations of the incident (i) and scattered (s) light.

(b) The power of the laser excitation was limited to 0.2 mW by the overheating effects. As in the case of orthorhombic ($Pnma$) $LaMnO_3$,[8] a higher laser power resulted in the appearance of strong background, shift of the lines towards lower wave numbers, and decrease of their intensity.

(c) The Raman line intensities were much lower compared to those of orthorhombic $LaMnO_3$.

The Raman spectra of rhombohedral $LaMnO_3$ as obtained with parallel and crossed scattering configurations are shown in Fig. 3. Five broad lines are observed at 179, 236, 329, 520, and 640 cm^{-1}. The first impression is that the spectra are more similar to those of orthorhombic $LaMnO_3$ (Ref. 8) than to the isostructural $LaAlO_3$. Based on the LDC it seems straightforward to assign four of the lines (these at 179, 236, 520, and 640 cm^{-1}) to the calculated 163-cm^{-1} E_g mode [pure La vibration in the hexagonal $(001)_h$ plane], 249-cm^{-1} A_{1g} mode (rotation of the oxygen octahedra around the hexagonal $[001]_h$ direction), 468-cm^{-1} E_g mode (pure oxygen bending vibration), and 646 cm^{-1} (out-of-phase stretching oxygen vibration), respectively. We will later argue, however, that although close in frequency to the expected E_g modes, the spectral structures near 520 and 640 cm^{-1} are of different origin.

We will first focus on the only A_{1g} mode allowed for the $R\bar{3}c$ phase. The vibrational pattern of this mode has the shape of the rhombohedral distortion (static rotational displacement of the oxygen octahedra around the hexagonal $[001]_h$ direction). With increasing temperature (approaching the temperature of the second-order structural transition to the cubic $Pm\bar{3}m$ phase) the mode frequency should soften to zero, i.e., this mode is one of the two ''soft'' modes. In

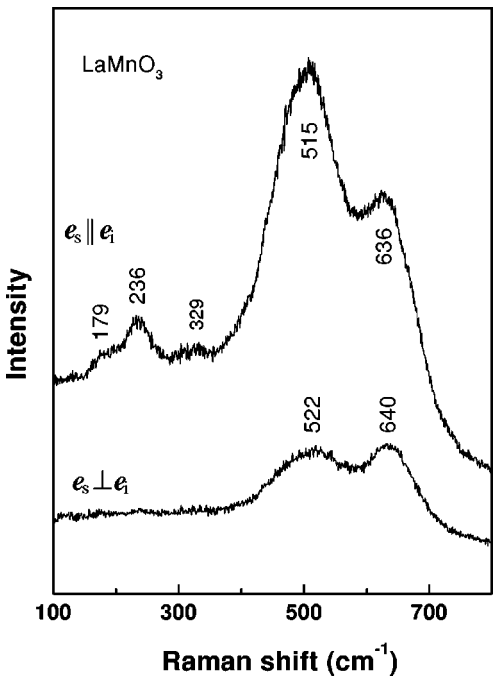

FIG. 3. Raman spectra of $LaMnO_3$ in parallel and crossed polarizations as obtained from a grain of unknown orientation. $\lambda_L = 632.8$ nm.

contrast, upon cooling the hardening of the A_{1g} mode has to be significantly larger than that of the the hardening of other modes caused solely by contraction of interatomic bonds. In other words, the frequency of the A_{1g} mode must correlate mainly with the rhombohedral distortion and depend only weakly on the change of the A-O and B-O distances in different ABO_3 perovskites with $R\bar{3}c$ structure. In the case of $LaMnO_3$ we assign the Raman line at 236 cm^{-1} to the A_{1g} mode based on the following facts:

(1) The results of LDC give for the A_{1g} mode the close wave number of 249 cm^{-1}.

(2) The angle of static rotation α is connected in a simple manner with the x parameter of the oxygen-site positions $(x,\bar{x}+1/2,1/4)$, namely,[15]

$$x = \frac{1}{2}\left(1 \pm \frac{1}{\sqrt{3}}\tan\alpha\right), \tag{4}$$

and can easily be calculated from the available crystallographic data. For example, in $RAlO_3$ (R=La,Pr,Nd), the A_{1g} mode frequency (at room temperature) shifts by factor 2 [from 122 cm^{-1} for R=La to 241 cm^{-1} for R=Nd (Ref. 10)] due to the increase of the rhombohedral distortion upon decrease of the radius of the R ion.[16] The direct comparison of the A_{1g} mode frequencies in $LaAlO_3$ (123 cm^{-1}) and $LaMnO_3$ (236 cm^{-1}) is also consistent with the above dependence. Indeed, using the values of $x=0.475$ for $LaAlO_3$ (Ref. 14) and $x=0.443$ for $LaMnO_3$,[6] one obtains $\alpha \approx 5°$ for $LaAlO_3$ and $\alpha \approx 11°$ for $LaMnO_3$, respectively.

(3) The large softening of the line observed recently in the Raman spectra of $La_{1-x}Sr_xMnO_3$ ($x=0.1$ to 0.3) by Podobedov *et al.*[17] from 240 cm^{-1} to 190 cm^{-1} (at room temperature) with increase of Sr content as well as the large hardening (about 20 cm^{-1}) upon cooling can also be explained by the change of the rhombohedral distortion with the Sr doping and the temperature, which is another proof of its origin as the ''soft'' A_{1g} mode.

It is worth noting that similar effects have been observed in the Raman spectra of perovskitelike compounds with more complicated orthorhombic distortion (Glazer's notation $a^-b^+a^-$, space group $Pnma$, $Z=4$).[8,18] In these compounds there are two types of static rotational displacements for the oxygen octahedra (around the x and y orthorhombic axis). This results in the existence of three Raman-active ''soft'' modes with orthorhombic A_g, B_{1g}, and B_{2g} symmetries, respectively. Comparing the spectra of more distorted $YMnO_3$ and less distorted orthorhombic $LaMnO_3$ Iliev *et al.* have observed a large shift of the only observed ''soft'' mode (A_g) from 396 cm^{-1} down to 284 cm^{-1}.[8] In the Raman spectra of $RTiO_3$ (R=La, Ce, Pr, Nd, Sm, Gd) Reedyk *et al.* also observed a large increase in frequency of one of the A_g lines, namely, from 287 cm^{-1} for $LaTiO_3$ to 385 cm^{-1} for $GdTiO_3$,[18] which also correlates with the increasing structural distortion.

The above-discussed dependence of the frequency of the soft modes on the rotational distortion has been known for a long time in the case of variation of distortion with temperature for a same compound[10] and has often been used to find the temperature of the structural transition. In addition we emphasize here that the observation of a large frequency shift of a given Raman line (compared to the shift of other lines) in a series of isostructural compounds at a fixed temperature is also a strong indication that the line with ''anomalous'' behavior corresponds to a ''soft'' mode. We will mention here that such ''anomalous'' lines have earlier been observed in a number of studies of isostructural series,[17,18] although other explanations have been proposed.

Now we will comment the two relatively strong broad Raman lines near 520 cm^{-1} and 640 cm^{-1}. In spite of closeness of their frequencies to the calculated values for two of the Raman-allowed E_g modes (468 cm^{-1} and 646 cm^{-1}) we will argue that these lines are not intrinsic for the ideal $R\bar{3}c$ structure. Indeed, their integrated intensity by far exceeds that of the A_{1g} line, while in the spectra of $LaAlO_3$ we have the opposite relationship. Furthermore, in the Raman spectra of doped $La_{1-x}Sr_xMnO_3$ ($x=0.1,0.2,0.3$) the intensity of these lines decreases with increasing Sr content.[17] Finally, Raman study of $La_{0.7}Ca_{0.3}MnO_3$ thin films deposited on $LaAlO_3$ substrate shows that these lines are pronounced only in the Raman spectra of the high-temperature insulating phase and completely disappear below the temperature of the insulator-metal transition ($T_c=260$ K).[19] These facts indicate that the modes under consideration are ''forbidden'' modes. We recall that the description of the structure using the $R\bar{3}c$ space group assumes six equal distances of the Mn-O bonds of MnO_6 octahedra. The oxygen octahedra around Mn^{+3} in the insulating $LaMnO_3$-type phases, however, are distorted due to the Jahn-Teller effect.[20] Recently a direct relationship has been established between the degree of the Jahn-Teller distortions of MnO_6 octahedra and conductivity and magnetic properties of the structure.[21] The intensity of these two lines in the Raman spectra of the rhombohedral $LaMnO_3$ correlates with the degree of the Jahn-Teller distortions of

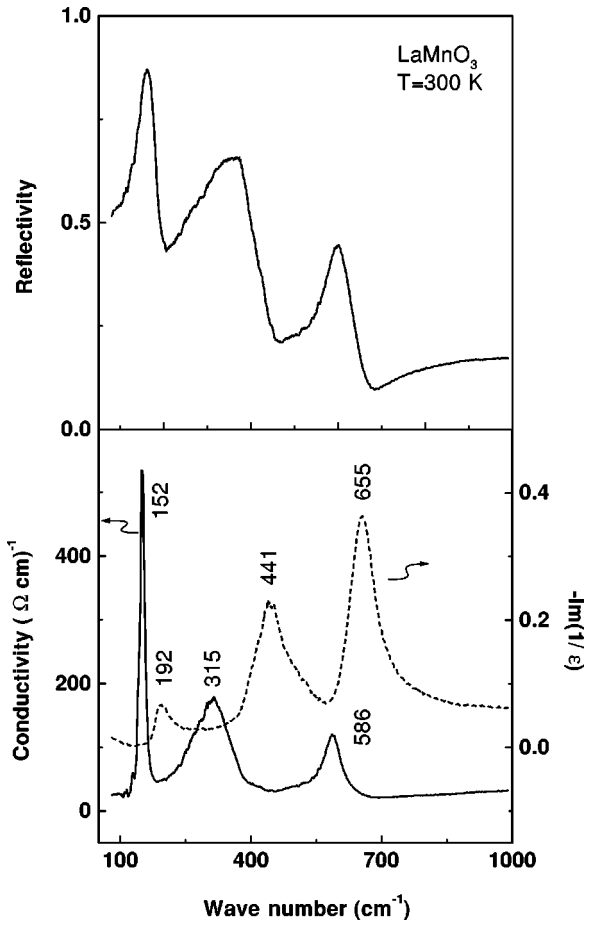

FIG. 4. Far-infrared reflectivity spectrum of $LaMnO_3$ (top) and calculated frequency dependence of the imaginary part of the dielectric function and the loss function (bottom).

the MnO_6 octahedra and they can be considered as Jahn-Teller–distortion-activated modes, otherwise forbidden for the $R\bar{3}c$ structure. They are reminiscent to the two strongest lines in the Raman spectra of the orthorhombic $LaMnO_3$,[8] corresponding to bending and stretching oxygen vibrations of the MnO_6 octahedra.

D. Infrared spectroscopy

The infrared absorption and reflectance spectra of ABO_3 (A=rare earth, B=transition metal or Al) in the infrared (IR) frequency range have been reported in several works. Earlier studies have been directed towards establishing the dependence of spectral features on the perovskite distortion.[22,23] More recently the interest in the optical properties of $LaAlO_3$ was renewed due mainly to the applications of this material as a suitable substrate for the growing of high-T_c superconducting films.[24–26] Due to the lack of LDC, however, the analysis of the far-infrared spectra and the assignment of the lines to definite phonon modes has been rather ambiguous. Having calculated the lattice dynamics of $LaAlO_3$ and $LaMnO_3$ (Table I) we can reanalyze and interpret available experimental data (see Fig. 4 and Table IV).

According to the symmetry, the following correlations hold between the long-wavelength IR-active $3A_{2u}$ and $5E_u$ modes of the rhombohedrally distorted $R\bar{3}c$ perovskites and phonons of the cubic $Pm3m$ perovskite structure compounds (see Table I and Fig. 1).

(a) Three A_{2u} and three out of five E_u modes make pairs and originate from the three zone-center triply degenerated IR-active F_{1u} modes of the ideal cubic perovskite. These three pairs correspond to (1) the low-frequency vibrations of Mn/Al-O sublattice against La atoms, (2) the middle-frequency bending vibrations of O and Mn/Al atoms, and (3) the high-frequency stretching vibrations of O and Mn/Al atoms.

Based on the origin of the pairs it is obvious that A_{2u}-E_u separation for a given pair is a measure of the deviation of the structure from the ideal cubic one. Given that the rhombohedral distortions are small, one expects that corresponding A_{2u}-E_u separation will also be relatively small (compared to, e.g., LO-TO splitting) and the three lines in question will dominate the infrared spectra of rhombohedral-structure ABO_3 compounds.

(b) The remaining two E_u modes in the rhombohedral phase make pairs with two inactive A_{1u} modes. These pairs originate from (1) a triply degenerated inactive (silent) $F_{2u}(\Gamma)$ mode at the Γ point of the cubic Brillouin zone (torsional oxygen vibrations of the oxygen octahedra) and (2) a triply degenerated mode of $F_{2g}(R)$ symmetry from the R point of the cubic Brillouin zone [vibrations of the Al (or Mn) atoms].

The facts that the latter modes are inactive in the parent cubic structure and the distortion of rhombohedral materials is small suggest that the corresponding bands in the IR spectra of rhombohedral perovskites will be relatively weak and their intensity will increase with the distortion. For one of the above-mentioned E_u modes, which involves predominantly the motions of Mn(Al), one expects a significant frequency shift $[\omega_{\mathrm{Al}}/\omega_{\mathrm{Mn}} \approx (m_{\mathrm{Mn}}/m_{\mathrm{Al}})^{1/2} = 1.43]$ for $LaAlO_3$ and $LaMnO_3$.

TABLE IV. Experimental and calculated TO frequencies (in cm^{-1}) of $LaAlO_3$. The data of Refs. 22 and 23 have been obtained from transmission measurements and those of Refs. 25 and 26 from the reflectivity.

Couzi *et al.* (Ref. 22)	Saine *et al.* (Ref. 23)	Calvani *et al.* (Ref. 25)	Zhang *et al.* (Ref. 26)	LDC This paper	Assignment
190	218	182	184	213 (A_{2u}) + 220 (E_u)	(Al + O)-La
				270 (E_u)	Torsional
440	460	429	428	366 (A_{2u}) + 371 (E_u)	Bending
525		501	496	481 (E_u)	Al
675	680	657 + 695	652 + 692	706 (A_{2u}) + 707 (E_u)	Stretching

An important result of the LDC of $LaAlO_3$ is that the separation of A_{2u}-E_u modes for a given pair is very small ($\leqslant 7$ cm^{-1}). This prediction is in qualitative agreement with experimental results on $LaAlO_3$,[25,26] where three strong ''restrahlen bands'' are observed in the far-infrared spectral range. The LO-TO splittings (up to 150 cm^{-1}) and phonon linewidths (up to 50 cm^{-1}) by far exceed the expected A_{2u}-E_u separation indeed.

Note also that an additional weak mode has been detected[25,26] in the spectra of $LaAlO_3$ around 500 cm^{-1}. We assign it to Al-related vibration that originates from the zone-boundary mode of cubic compound. The position of this mode is in reasonable agreement with the results of calculations (Table IV). An additional piece of evidence for this mode being metal related comes from the fact that in the infrared spectrum of $LaCoO_3$ there are no features around 500 cm^{-1}, while a band exists[27] around 328 cm^{-1}, which even at room temperature shows signs of splitting into two components, presumably A_{2u} and E_u modes. The ratio of corresponding wave numbers $500/328=1.52$ is very close to the value of 1.48 expected from simple mass considerations $[(\omega_{Al}/\omega_{Co} \approx (m_{Co}/m_{Al})^{1/2}=1.48]$.

The room-temperature reflectivity spectrum obtained from the polished surface of $LaMnO_3$ ceramics as well as the spectral dependence of the conductivity and loss function as calculated by Kramers-Kronig analysis are shown in Fig. 4. Our experimental results are in good agreement with previously published data on the infrared spectra of undoped[28] and doped[29,30] rhombohedral $LaMnO_3$. Three main bands with TO/LO frequencies of 152/192, 315/441, and 586/655 cm^{-1} dominate the spectra. As in the case of isostructural $LaAlO_3$, we assign these bands to the three A_{2u}-E_u pairs originating from the cubic $F_{1u}(\Gamma)$ modes (see Table I for comparison of the wave numbers). The rhombohedral distortion-induced doublet structure of these bands could not be clearly resolved even for the middle-frequency band, where the largest A_{2u}-E_u splitting of about 40 cm^{-1} is predicted by LDC. It implies that the two remaining E_u bands are either too weak or overlap with the stronger bands. In particular, an overlap might occur for the E_u(Mn) mode and the middle-frequency A_{2u}-E_u pair, expected at 310–320 cm^{-1}.

IV. CONCLUSION

In summary, we studied the Raman and infrared phonons of isostructural rhombohedral $LaMnO_3$ and $LaAlO_3$ and made an assignment of the experimentally observed lines to definite atomic vibrations based on the symmetry considerations of rhombohedral and parent cubic structures and by comparison with the results of lattice-dynamical calculations. The soft mode related to the rhombohedral distortions in $LaMnO_3$ was unambiguously identified. We also showed that the broad Raman bands in the high-frequency phonon range of the rhombohedral $LaMnO_3$ are not proper modes of the $R\bar{3}c$ structure, but are rather induced by the dynamic Jahn-Teller effect.

ACKNOWLEDGMENTS

M.V.A. acknowledges the financial support from the Alexander von Humboldt Foundation (Bonn, Germany). This work was supported in part by Grant No. F530 (NIS 2241) of the Bulgarian National Science Fund, the State of Texas through the Texas Center of Superconductivity at the University of Houston, and by the NSF through the Material Research Science and Engineering Center at the University of Houston.

*Permanent address: Faculty of Physics, University of Sofia, BG-1164 Sofia, Bulgaria.

[1] P. Schiffer, A. P. Ramirez, W. Bao, and S.-W. Cheong, Phys. Rev. Lett. **75**, 3336 (1995).
[2] C. Zener, Phys. Rev. **82**, 403 (1951); P. W. Anderson and H. Hasegawa, *ibid.* **100**, 675 (1955); P. G. de Gennes, *ibid.* **118**, 141 (1960).
[3] A. J. Millis, P. B. Littlewood, and B. I. Shraiman, Phys. Rev. Lett. **74**, 5144 (1995).
[4] G. Zhao, K. Conder, H. Keller, and K. A. Müller, Nature (London) **381**, 676 (1996).
[5] P. Norby, I. G. Krogh Andersen, and E. Krogh Andersen, J. Solid State Chem. **119**, 191 (1995).
[6] Q. Huang, A. Santoro, J. W. Lynn, R. W. Erwin, J. A. Borchers, J. L. Peng, and R. L. Greene, Phys. Rev. B **55**, 14 987 (1997).
[7] V. B. Podobedov, A. Weber, D. B. Romero, J. P. Rice, and H. D. Drew, Phys. Rev. B **58**, 43 (1998).
[8] M. N. Iliev, M. V. Abrashev, H. G. Lee, V. N. Popov, Y. Y. Sun, C. Thomsen, R. L. Meng, and C. W. Chu, Phys. Rev. B **57**, 2872 (1998).
[9] A. M. Glazer, Acta Crystallogr., Sect. B: Struct. Crystallogr. Cryst. Chem. **B28**, 3384 (1972).
[10] J. F. Scott, Phys. Rev. **183**, 823 (1969).
[11] G. N. Zhizhin, B. N. Mavrin and V. F. Shabanov, in *Optical Vibrational Spectra of Crystals* (Nauka, Moscow, 1984), p. 212 (in Russian).
[12] V. N. Popov, J. Phys.: Condens. Matter **7**, 1625 (1995).
[13] C. R. A. Catlow, W. C. Mackrodt, M. J. Norgett, and A. M. Stoneham, Philos. Mag. **35**, 177 (1977).
[14] C. de Rango, G. Tsoucaris and C. Zelwer, Acta Crystallogr. **20**, 590 (1966).
[15] Zheng Wen-Chen, J. Phys.: Condens. Matter **7**, 4499 (1995).
[16] R. W. G. Wickoff, *Crystal Structures* (Interscience Publishers, John Wiley & Sons, New York, 1964), Vol. 2, p. 412.
[17] V. B. Podobedov, A. Weber, D. B. Romero, J. P. Rice, and H. D. Drew, Solid State Commun. **105**, 589 (1998).
[18] M. Reedyk, D. A. Crandles, M. Cardona, J. D. Garrett, and J. E. Greedan, Phys. Rev. B **55**, 1442 (1997).
[19] M. V. Abrashev *et al.* (unpublished).
[20] P. G. Radaelli, M. Marezio, H. Y. Hwang, S-W. Cheong, and B. Batlogg, Phys. Rev. B **54**, 8992 (1996); P. G. Radaelli, G. Iannone, M. Marezio, H. Y. Hwang, S-W. Cheong, J. D. Jorgensen, and D. N. Argyriou, *ibid.* **56**, 8265 (1997).
[21] C. H. Booth, F. Bridges, G. H. Kwei, J. M. Lawrence, A. L. Cornelius, and J. J. Neumeier, Phys. Rev. Lett. **80**, 853 (1998).
[22] M. Couzi and P. V. Huong, J. Chim. Phys. Phys.-Chim. Biol. **69**, 1339 (1972).
[23] M. C. Saine, E. Husson, and H. Brusset, Spectrochim. Acta A **37**, 985 (1981).
[24] D. van der Marel, H. -U. Habermeier, D. Heitmann, W. König,

and A. Wittlin, Physica C **176**, 1 (1991).
[25] P. Calvani, M. Capizzi, F. Donato, P. Dore, S. Lupi, P. Maselli, and C. P. Varsamis, Physica C **181**, 289 (1991).
[26] Z. M. Zhang, B. I. Choi, M. I. Fink, and A. C. Anderson, J. Opt. Soc. Am. B **11**, 2252 (1994).
[27] S. Tajima, A. Masaki, S. Ushida, T. Matsuura, K. Fueki, and S. Sugai, J. Phys. C **20**, 3469 (1987).
[28] L. Kebin, L. Xijun, Z. Kaigui, Z. Jingsheng, and Z. Yuheng, J. Appl. Phys. **81**, 6943 (1997).
[29] K. H. Kim, J. Y. Gu, H. S. Choi, G. W. Park, and T. W. Noh, Phys. Rev. Lett. **77**, 1877 (1996).
[30] Y. Okimoto, T. Katsufuji, T. Ishikawa, T. Arima, and Y. Tokura, Phys. Rev. B **55**, 4206 (1997).